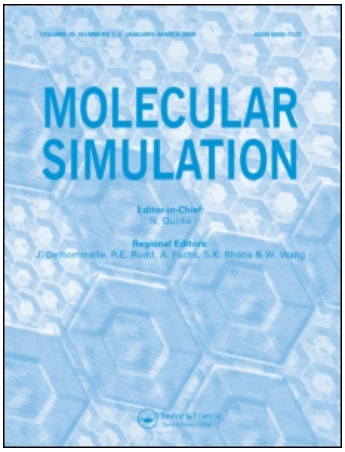

Molecular Simulation
Publication details, including instructions for authors and subscription information:
http://www.informaworld.com/smpp/title~content=t713644482

Simulations on the Primitive Electrolyte Environment of a High Charge-density Polyelectrolyte. A Sampling Problem and its Solution

Heather Gordon[a]; Saul Goldman[a]
[a] Guelph-Waterloo Centre for Graduate Work in Chemistry Guelph Campus Guelph, Ontario, Canada

To cite this Article Gordon, Heather and Goldman, Saul(1989) 'Simulations on the Primitive Electrolyte Environment of a High Charge-density Polyelectrolyte. A Sampling Problem and its Solution', Molecular Simulation, 3: 4, 213 — 225
To link to this Article: DOI: 10.1080/08927028908031374
URL: http://dx.doi.org/10.1080/08927028908031374

Molecular Simulation, 1989, Vol. 3, pp. 213–225
Reprints available directly from the publisher
Photocopying permitted by license only

SIMULATIONS ON THE PRIMITIVE ELECTROLYTE ENVIRONMENT OF A HIGH CHARGE-DENSITY POLYELECTROLYTE. A SAMPLING PROBLEM AND ITS SOLUTION

HEATHER GORDON AND SAUL GOLDMAN

Guelph-Waterloo Centre for Graduate Work in Chemistry Guelph Campus Guelph, Ontario Canada N1G 2W1

(*Received August, 1988; in final form November, 1988*)

We show that the classical Metropolis Monte Carlo (MMC) algorithm converges very slowly when applied to the primitive electrolyte environment for a high charge-density polyelectrolyte. This slowness of convergence, which is due to the large density inhomogeneity around the polyelectrolyte, produces noticeable errors in the ion distribution functions for MMC runs of 1.3×10^6 trial steps started from nonequilibrium distributions. We report that an algorithm which we call DSMC (for density-scaled Monte Carlo) overcomes this problem and provides relatively rapid convergence in this application. We suggest that DSMC should be well-suited for other Monte Carlo simulations on physical systems where large density inhomogeneities occur.

KEY WORDS: Electrolyte, density inhomogeneity, scaled Monte Carlo

1. INTRODUCTION

The important influence of dissolved electrolyte, near a high charge-density polyelectrolyte such as DNA, on its conformational, thermodynamic and binding characteristics is well-established [1–7]. It is also well-established [4–11] that counterion concentrations next to such a polyelectrolyte are about two orders of magnitude higher than at large distances (a few hundred angstroms) from the polyelectrolyte surface. This interesting state of affairs has attracted the attention of theoreticians. One basic theoretical problem is to quantitatively account for the variation of electrolyte concentration with distance from the surface of the polyelectrolyte. To this end, the counterion condensation theory [3, 12, 13], the Poisson–Boltzmann equation [14–18], and the hypernetted chain approximation [19–21] have been used. These calculations involve the so-called primitive electrolyte model [22, 23] wherein the ions of the electrolyte are "dissolved" in a dielectric continuum.

The accuracy of these theories have been assessed by comparison with Monte Carlo simulations [24–29]. While the methodology of these simulations has become routine in applications to homogeneous condensed phases involving short-range interactions, there are two particular difficulties associated with applications to the polyelectrolyte problem. One problem is how to properly include long-range coulombic interactions in the simulation. An acceptable approximation for doing this has been worked out in the last few years [24, 25, 30]. A second problem, which has not been previously addressed, stems from the very large inhomogeneity of the counterion density. The resolution of this second problem is the basis of this article.

As noted previously, the counterion concentration varies by some two orders of magnitude between distances close to the polyelectrolyte surface and those several hundred angstroms away (Figures 1 and 2). This creates severe sampling inefficiency for simulations carried out using a traditional sampling cube [31]. We will show that this sampling inefficiency, because it slows the convergence rate of the simulation, can lead to significant inaccuracy in the simulated counterion (and coion) distribution functions, even for fairly long runs.

In the traditional Metropolis method [31], and also in the more recent force-biased Monte Carlo method [32, 33], a cube of fixed size is used to constrain the maximum displacement that can occur on a trial move. Thus, a sampling cube that efficiently samples configuration space next to the polyelectrolyte, where the counterion density is $O(1\ \text{mol/dm}^3)$, will do a poor job far from the polyelectrolyte surface, where the density is $\leq O(.01\ \text{mol/dm}^3)$, and vice versa. Similarly, Smart Monte Carlo [34], while making use of variable maximum displacements, does not relate these displacements to the local density, and so would not be expected to alleviate this sampling problem.

A different Monte Carlo algorithm previously called ESDMC (for energy-scaled

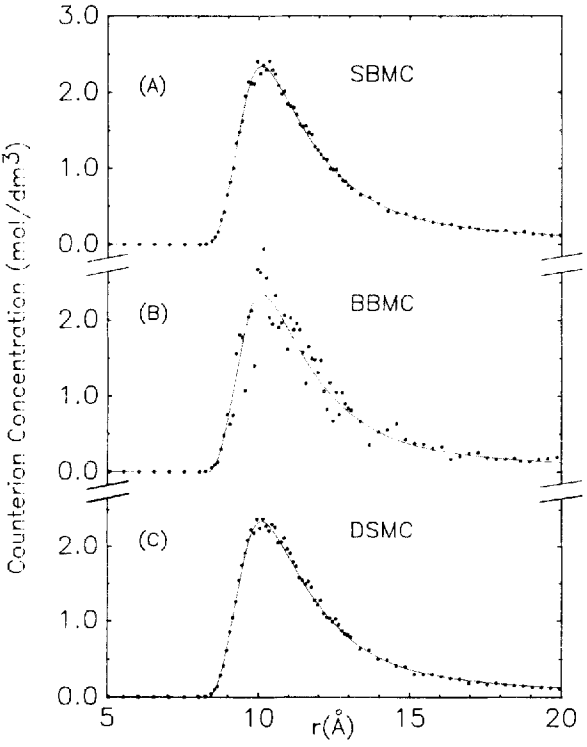

Figure 1 Comparison of Sampling Techniques: counterion concentration versus radial distance r from the polyion center at close distances. Points (●) are simulation results for 1.3×10^6 trial steps. Here, and in Figures 2 and 3, each point is an average over an annulus that is 0.1 Å thick. Some data points have been omitted for clarity. In each Figure, the solid line is from a least-squares spline fit to the 3.726×10^6 trial step DSMC distribution function (see text). (A) SBMC:MMC with $\Delta_0 = 5$ Å; (B) BBMC:MMC with $\Delta_0 = 100$ Å; (C): DSMC (Δ_0 given by equation (6) with K = 100 Å).

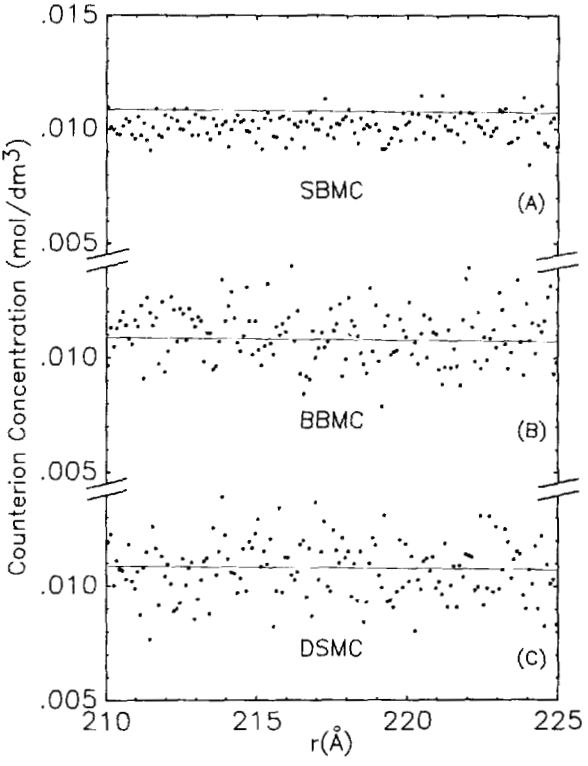

Figure 2 Counterion concentration versus radial distance r from polyion center at far distances. All symbols are as in Figure 1.

displacement Monte Carlo) [35–37] can be used to overcome this inefficiency. We show that this algorithm, when appropriately applied, leads to relatively rapid convergence of the counterion distribution function at all distances from the polyelectrolyte surface.

The ESDMC algorithm suffered an inauspicious beginning. In the original formulation [35], it contained an error. This error stemmed from the assumption that detailed balance was satisfied, whereas later work showed that it was not [36]. Subsequently, the algorithm was corrected, so as to satisfy detailed balance, but the corrected version proved slow to converge when applied to a dense Lennard-Jones fluid [37]. The ESDMC algorithm, which we re-name DSMC (for density-scaled Monte Carlo), is ideally suited to the present problem however, since it allows for a constraining cube whose size can be scaled (i.e. varied) to smoothly sample over the inhomogeneity. The original algorithm (as its original name implies) involved scaling the size of the constraining cube to the potential energy of the particle. For the problem at hand, we will scale the size of this cube with the distance of the trial ion from the polyelectrolyte. Ions near the polyion surface, where the density is high, will be constrained to small trial steps; for those far away where the density is low, the trial steps will be large. We will show that this leads to efficient sampling of configuration

space at all distances and therefore in all regions around the polyelectrolyte. We will also show that, as a consequence of this gain in sampling efficiency, the rate at which the counterion distribution function converges to the correct limit, is much faster with DSMC than with MMC.

2. THEORY

The rules derived below have been given elsewhere [37]. However, for the sake of completeness and because the derivation in reference 37 referred to scaling with respect to energy (as opposed to location), we repeat some of the derivation here. The set of rules that are used to make the acceptance-rejection decision for each new trial configuration is based on the condition of detailed balance, which ensures that any arbitrary initial distribution function will eventually converge to the correct limiting distribution [38]. Thus, if $\{f_i\}$ is the normalized limit (equilibrium) distribution and p_{ij} is the probability of the system undergoing a transition from state "i" to state "j", detailed balance requires that:

$$f_i p_{ij} = f_j p_{ji}, \qquad i \neq j \tag{1}$$

Writing p_{ij} as the product of an a priori normalized transition probability p_{ij}^* and an acceptance probability a_{ij} gives:

$$f_i p_{ij}^* a_{ij} = f_j p_{ji}^* a_{ji} \tag{2}$$

We consider only single particle moves, so that the two states "i" and "j" differ only in the location of one particle. Also, we are not force-biasing the moves, so that each trial location that is generated in an attempted move, is selected randomly from the space inside the initial constraining cube. Since the size of the constraining cube will be made to vary with distance of the trial particle from the surface (or axis) of the polyelectrolyte, the cubes drawn around a trial particle in states "i" and "j" will usually differ in size. Therefore, we start by considering all the possible overlap conditions that can, under the most general conditions, arise: (1) $p_{ij}^* > 0$ and $p_{ji}^* > 0$ (complete overlap); (2) either $p_{ij}^* > 0$ and $p_{ji}^* = 0$ or $p_{ji}^* > 0$ and $p_{ij}^* = 0$ (partial overlap); (3) $p_{ij}^* = p_{ji}^* = 0$ (zero overlap). For the complete overlap condition, the constraining cube drawn around the particle in the trial location encompasses the coordinates of the location of the particle in the initial state, while in the partial overlap condition, it does not. We note that the zero overlap condition will not arise operationally, and so does not lead to a rule; it automatically satisfies detailed balance. Also, the only partial overlap condition that will arise here, is the $p_{ij}^* > 0$ and $p_{ji}^* = 0$ combination.

To satisfy equation (2) for the case of complete overlap we rearrange it to the form:

$$\frac{a_{ij}}{a_{ji}} = \frac{f_j}{f_i}\frac{p_{ji}^*}{p_{ij}^*} \tag{3}$$

and use the fact that

$$\frac{p_{ji}^*}{p_{ij}^*} = \frac{V_i}{V_j} \tag{4}$$

where V_i and V_j are the volumes of the constraining cubes in states "i" and "j" respectively. Equation (4) uses the fact that the number of states available at each step

is the same as the number of distinguishable locations inside the constraining cube. Using equation (4) in equation (3) gives:

$$\frac{a_{ij}}{a_{ji}} = \frac{f_j}{f_i}\frac{V_i}{V_j} = Q \tag{5}$$

This leads to the following rule for the condition of complete overlap: If $Q \geqq 1$ accept the new state, i.e. set $a_{ji} = Q^{-1}$ and $a_{ij} = 1$; if $Q < 1$, accept the new state with probability Q, i.e. set $a_{ji} = 1$ and $a_{ij} = Q$.

When partial overlap occurs ($p_{ij}^* > 0$ and $p_{ji}^* = 0$) the rule is always to reject the new state and count the initial state again in the averaging process; i.e. we satisfy equation (2) by setting $a_{ij} = 0$.

The extra computational expense incurred at each trial step for the calculation of the volumes of the constraining cubes V_i and V_j, is totally negligable. Therefore each trial step for DSMC consumes almost exactly the same amount of computer time as one for MMC.

It remains to specify a rule for how the size of the constraining cube is to vary with distance from the polyelectrolyte. We somewhat arbitrarily used:

$$\Delta_0 = \left(\frac{K}{R}\right) r_{ip} \tag{6}$$

where Δ_0 is the maximum displacement in either direction, along each cartesian coordinate, r_{ip} is the radial distance of the selected ion from the axis of the polyelectrolyte, R is the distance of the outer boundary of the cylindrical simulation cell from the axis of the polyelectrolyte (here 225 Å) and K is chosen so as to make the acceptance rate *at all distances* fall within the range 0.3–0.6. Thus K was taken as 100 Å (Table 2). This choice provides a constraining cube whose volume ($8\Delta_0^3$), varied in operation from $\sim 3.6 \times 10^2$ Å^3 at $r_{ip} = 8$Å, to 8×10^6 Å^3 at $r_{ip} = 225$Å.

3. CALCULATIONS

(a) Model

The polyelectrolyte (or polyion) was taken to be an infinitely long, rigid, soft cylinder, with a uniform axial charge density of $-e/b$, where "e" is the electronic charge and "b" is the length of a segment of the axis that holds exactly a unit of charge. To mimic DNA [24, 25], a high charge-density polyion, we took "b" to be 1.7 Å. The small ions (those in solution around the polyion) were taken to be Lennard-Jones spheres with an embedded point charge. A Lennard-Jones ion-polyion potential was used to model the non-coulombic part of the interaction and to exclude small ions from the center of the cylinder surrounding the axial charge. The Lennard-Jones parameters were selected so that the minimum of the polyion-counterion potential occurred at 10 Å, and that of the positive ion-negative ion potential occurred at 2.76 Å. These minima were chosen because they coincided with values used previously [24]. At a crude level, the ion-polyion potential mimics some of the features of double-stranded DNA in water [24, 25]. Our Lennard-Jones parameters are given in Table 1. To avoid unnecessary complications, we took the negative and positive small ions to have the same values of the Lennard-Jones parameters. The dielectric constant of the continuum solvent was taken to be 78. 358, which is the value of water at 25°C and 1 atmosphere.

Table 1 Lennard-Jones parameters for ion-ion and ion-polyion interactions.

	$\varepsilon_{LJ}(erg)$	$\sigma_{LJ}(\AA)$
ion-ion	54.356×10^{-16}	2.73
ion-polyion	20.20×10^{-16}	11.365

(b) Simulation cell

The simulation cell was a cylinder whose outer wall was concentric around the cylindrical polyion; the axis of the polyion was also the axis of the simulation cell. Thus the small ions were confined to a cylindrical annulus, whose outer wall (the outer cylindrical surface of the simulation cell) was taken to be impenetrable. To make the number of small ions finite, we used periodic boundary conditions in the z-direction, where the z-direction was taken to be along the polyion axis. We took the length of the simulation cell to be 102 Å and the radius, R, 225 Å.

We used a total of 260 univalent small ions in the central cell. Sixty of these were positively charged counterions required to neutralize the charge on the polyion segment contained in the simulation cell. The remaining 200 univalent ions (100 positive, 100 negative) constituted the "added salt" or "supporting electrolyte". This added salt concentration, 200 ions over the volume of the simulation cell, corresponds to .0102 mol/dm^3 of supporting electrolyte.

(c) Potential energy

The total potential energy of an ion "i" was obtained by summing the contributions from interactions inside and outside the simulation cell. The internal contribution was obtained from:

$$u_i^{\text{int}} = \sum_{j \neq i} (u_{ij}^{LJ} + u_{ij}^{\text{coul}}) + u_{ip}^{LJ} + u_{ip}^{\text{coul, int}} \tag{7}$$

where

$$u_{ij}^{\text{coul}} = \frac{Z_i Z_j e^2}{\varepsilon_0 r_{ij}}$$

$$u_{i\alpha}^{LJ} = 4\varepsilon_{i\alpha}\left[\left(\frac{\sigma_{i\alpha}}{r_{i\alpha}}\right)^{12} - \left(\frac{\sigma_{i\alpha}}{r_{i\alpha}}\right)^{6}\right] \qquad \alpha = \begin{matrix} i \text{ for small ions} \\ p \text{ for the polyion} \end{matrix}$$

and

$$u_{ip}^{\text{coul, int}} = \frac{-2Z_i e^2}{\varepsilon_0 b} \ln\left\{\frac{L}{2r_{ip}} + \left[1 + \left(\frac{L}{2r_{ip}}\right)^2\right]^{\frac{1}{2}}\right\}$$

In the above, ε_0 is the dielectric constant, r_{ij} is the ion-ion distance, Z_i, is the valence (here ± 1), and the symbols b, r_{ip}, and L are as defined previously.

The external contribution was obtained from:

$$u_i^{\text{ext}} = u_{ip}^{\text{coul, ext}} + u_{i\text{-si}}^{\text{ext}} \tag{8}$$

In equation 8, $u_{ip}^{\text{coul, ext}}$ and $u_{i\text{-si}}^{\text{ext}}$ are respectively, the selected ion's interaction energy with the polyion and the small-ion charge distribution, both external to (above and below)

the central cell. The z coordinate of the selected ion is always zero since the vertical center of the simulation cylinder is re-set to zero for every state sampled. As in other work [25] we used:

$$u_{ip}^{\text{coul, ext}} = \frac{2Z_i e^2}{\varepsilon_0 b} \ln(r_{ip}) + \frac{2Z_i e^2}{\varepsilon_0 b} \ln\left\{\frac{L}{2r_{ip}} + \left[1 + \left(\frac{L}{2r_{ip}}\right)^2\right]^{1/2}\right\} \tag{9}$$

$$u_{\text{i-si}}^{\text{ext}} = \frac{-2Z_i e}{\varepsilon_0} \int_0^R \varrho_{\text{ext}}(r') r' dr' \int_0^{2\pi} \ln\left\{\frac{L}{2} + \left[1 + \left(\frac{L}{2}\right)^2 + r_{ip}^2 + r'^2 - 2r_{ip} r' \cos\phi'\right]^{\frac{1}{2}}\right\} d\phi \tag{10}$$

In equation 10, $\varrho^{\text{ext}}(r')$ is the net charge density due to small ions outside the simulation cell at a distance r' from the polyelectrolyte axis. As explained in section (d), it was obtained from the charge density inside the central cell [30, 24–27], which is generated during the simulation.

The double integration in equation 10 was done by compound Gauss-Legendre quadrature, and the charge density at the Gauss points was obtained by Lagrange interpolation.

Equations (7) through (10) contain the implicit assumption that the dielectric constant within the rigid polyion rod is ε_0, the same as that of the continuum solvent. This convention, while artificial, is inherent in the use of the primitive electrolyte model, and was used with all the algorithms.

(d) Simulations

We used the same pre-determined external charge density $\varrho_{\text{ext}}(r')$, in equation 10, for all the runs for which we compared convergence rates. We did this so as not to obscure the effect we wished to illustrate, namely the very different convergence rates obtained from different algorithms for the ion distribution functions inside the central cell. We obtained $\varrho_{\text{ext}}(r')$ from a long simulation using the DSMC algorithm. Specifically $\varrho_{\text{ext}}(r')$ was obtained from the average taken during a collection run of 3.726×10^6 trial steps. The collection run was preceded by a pre-equilibration run of 1.6×10^6 trial steps. This latter run was started from a uniform external charge density and a semi-random interval ion distribution. By semi-random we mean that the ions were randomly placed in the cylindrical annulus of the central cell, but overlaps with other ions, the polyion and the external cylindrical wall were avoided. The averaged $\varrho_{\text{ext}}(r')$ of the pre-equilibration run was used to construct the starting $\varrho_{\text{ext}}(r')$ for the collection run. During both the pre-equilibration and the collection runs, $\varrho_{\text{ext}}(r')$ was periodically up-dated by setting it equal to the cumulatively averaged $\varrho_{\text{int}}(r')$. Also, as mentioned before, the function we used for $\varrho_{\text{ext}}(r')$ in the comparative study described below was an average of the periodic updates in the collection run.

We carried out convergence rate studies of the small-ion distribution functions for Metropolis Monte Carlo (MMC) and DSMC. The DSMC calculation was done using equation 6 and the parameters described with it. We did two runs using MMC; one with a small maximum displacement ($\Delta_0 = 5$ Å) and another with a large maximum displacement ($\Delta_0 = 100$ Å). We will refer to these runs as SBMC and BBMC for "small box Monte Carlo" and "big Monte Carlo" respectively.

The DSMC, SBMC and BBMC all had the same starting configuration (semi-

random, as described above), and the same (unvarying) external charge density $\varrho_{ext}(r')$. Each run involved 1.3×10^6 trial steps and consumed approximately the same amount of computer time.

4. RESULTS

Our results are given in Table 2 and in Figures 1–4. An examination of the acceptance rates given in Table 2 for the MMC runs illustrates the problem that prompted this work. From the entries in column 3, we see that, although the overall BBMC acceptance rate is ~ 0.5, the acceptance rates for particles close to the polyelectrolyte surface are extremely low; only about 1 trial step in 50 is accepted there. This is a possible indication of slow equilibration in this region. Although the SBMC algorithm (column 2) produces acceptance rates of 0.4–0.5 near the surface of the polyion, it also produces very high acceptance rates ($> .9$) in regions far from the polyion surface. This is also suggestive of slow equilibration, since these high acceptance rates are a consequence of the small volume sampled at each step relative to the large mean free path between ions in the bulk primitive electrolyte solution. It is seen from the entries in column 4 however, that the DSMC algorithm provides acceptance rates that are generally considered "reasonable" (i.e. 0.3–0.6) at all distances from the surface of the polyelectrolyte. The results displayed in Figures 1–4 strongly support

Table 2 Comparison of MMC and DSMC for Runs of 1.3×10^6 Trial Steps

Acceptance rates[d] *Radial Dimensions of Annuli (Å)*	*MMC*		
	SBMC[a]	*BBMC*[b]	*DSMC*[c]
5–10	.428	.018	.310
10–15	.490	.022	.346
15–20	.793	.098	.427
20–25	.855	.205	.456
25–35	.911	.407	.497
35–55	.942	.636	.515
55–75	.961	.755	.537
75–100	.959	.771	.530
100–140	.965	.762	.532
140–180	.960	.653	.494
180–225	.938	.458	.328
5–225 (Overall)	.885	.516	.435
Rejection Rates			
Hard Boundary[e]	.008	.171	.130
Inaccessible States[f]	–	–	.204
Bulk Concentrations (mol/dm^3)[g]			
counterions	.0101(± .0001)	.0109(± .0001)	.0106(± .0001)
coions	.0086(± .0001)	.0108(± .0001)	.0106(± .0001)

[a] SBMC means MMC with $\Delta_0 = 5$ Å
[b] BBMC means MMC with $\Delta_0 = 100$ Å
[c] DSMC with Δ_0 from equation (6); $K = 100$ Å
[d] Acceptance rate is ratio of trial moves accepted to total of attempted moves starting from a position within annuli shown.
[e] Rejection rate due to ions hitting hard outer boundary at R = 225 Å.
[f] Rejection rate in DSMC due to initial states being inaccessible from trial states.
[g] These concentrations are averages taken over the outer 15 Å next to the outer cylindrical wall of the simulation cell. The errors are standard deviations of the averages. The results for the long DSMC runs were .0108(± .0001)mol/dm^3 for counterions and .0106(± .0001)mol/dm^3 for coions.

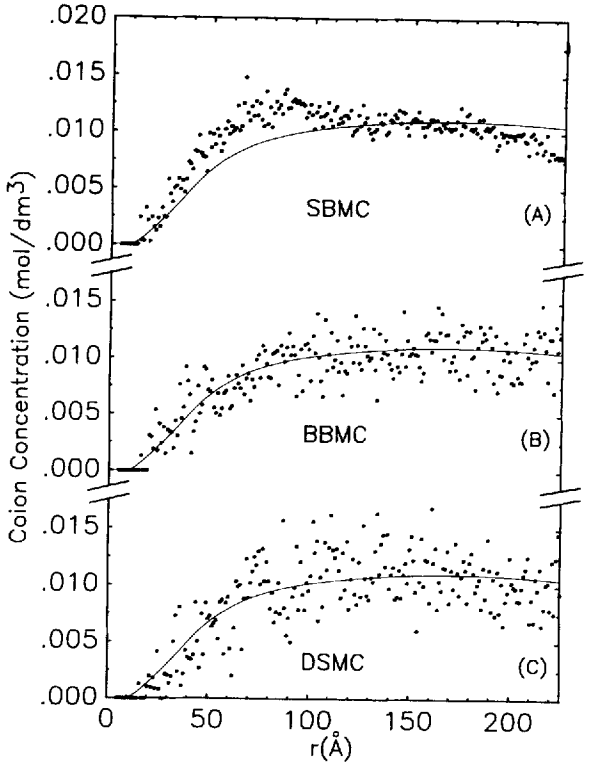

Figure 3 Coion concentration versus radial distance r from polyion center. All symbols as in Figure 1. Some data points have been omitted for clarity. The downward curvature at large r in the solid curve is due to the particular functional form used in our spline fit and has no theoretical significance.

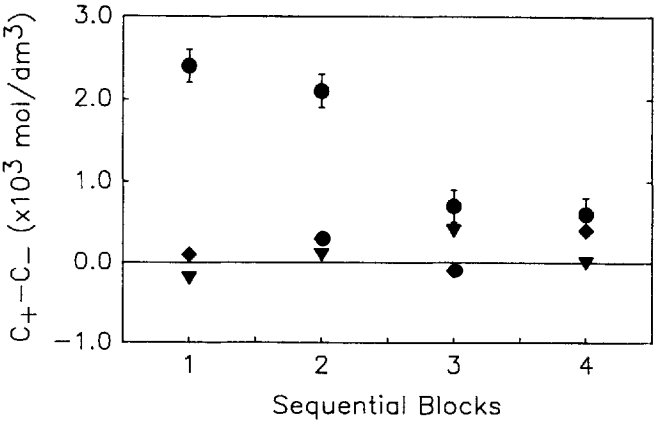

Figure 4 Excess bulk postive ion concentration ($C_+ - C_-$) for sequential blocks of trial steps. Each block represents 3.25×10^5 trial steps. The bulk counter- and coion concentrations C+ and C_-, are averages taken over the outer 15 Å adjacent to the cylindrical wall of the simulation cell. (●): SBMC; (◆): BBMC; (▼): DSMC. The error bars were calculated from the standard deviations of the means of C_+ and C_-. They are about twice as large as those of SBMC data and, for each point, encompass zero.

the above suggestion of slow convergence associated with either the low or the high acceptance rates of the MMC algorithm.

The solid curve in Figures 1–3 is from a least-squares spline fit to the distribution functions obtained from the 3.726×10^6 trial step DSMC run described in section 3(d). While it is not possible to be absolutely certain, we believe, for a variety of reasons, that these solid curves do in fact represent the correct limiting answers for this system. First, this simulation was extensively pre-equilibrated (3(d)). Second, this was a relatively long run — almost three times longer than our subsequent 1.3×10^6 step comparative runs, which were not pre-equilibrated. Third, our bulk ion concentrations, i.e. those at the furthest distances from the polyion (210–225 Å), are statistically identical to those reported in reference 24 (0.01074 mol/dm^3 from run B, Table III, reference 24 versus 0.0108($\pm$0.0001)mol/dm^3 and 0.0106($\pm$0.0001)mol/dm^3 for counter- and coions, respectively, from our work), where the same polyion charge density, dielectric constant, temperature, system size and numbers of small ions were used. This last point is strongly confirmatory, because the calculation in reference 24 involved a different starting small ion distribution from that used here.

From Figure 1 we see that the counterion distribution function near the polyelectrolyte surface is, for the same run length, much more scattered with the BBMC algorithm than with SBMC or DSMC. Specifically, the root-mean-square deviations from the solid curve were: SBMC = 0.089, DSMC = 0.066, BBMC = 0.446. These values were, in each case, calculated from eleven points that were within 0.5 Å of the center of the counterion peak. Therefore a much longer simulation run would be required for the BBMC algorithm to give the peak with the same precision as obtained from either the SBMC or DSMC algorithms.

Figure 2 is a plot of the counterion distribution functions at far distances from the polyion. While both the BBMC and DSMC results are distributed symmetrically about the value 0.0108 mol/dm^3 (from the 3.726×10^6 trial step DSMC run), the SBMC results are not. Despite the smaller scatter of the SBMC results the accuracy of the bulk counterion concentration is not as good as that found using the BBMC or DSMC algorithms.

Figure 3 shows that the coion distribution function from the SBMC algorithm is incorrectly skewed at intermediate and large distances. This last problem is also reflected in the poor result obtained from the SBMC algorithm for the bulk coion concentration (0.0086($\pm$0.0001)mol/dm^3). This value is significantly different from 0.0106 mol/dm^3 found both by the long DSMC run and by the work reported in reference 24. Moreover, *significantly different* positive and negative ion concentrations near the outer wall were obtained from SBMC (Table 2). Theory and simulations concur [24], that the concentrations of counter- and coions should be equal at these distances, for this model system. In Figure 4, we plot the deviation from electroneutrality near the outer wall for the SBMC, BBMC and DSMC simulations. The difference between the average counterion and coion concentrations over the most distant 15 Å of the cell were calculated for four separate, sequential blocks, each of 3.25×10^5 trial steps. For both DSMC and BBMC, the condition of electroneutrality is maintained (within statistical error), starting from the first block. For the SBMC simulation, there persists a significant excess of positive charge, even after four blocks.

Thus, for a run length of 1.3×10^6 trial steps, only the DSMC algorithm provides consistently satisfactory results at all distances from the polyelectrolyte surface, for both coions and counterions. An MMC algorithm with small maximum step sizes

does not efficiently sample regions of low particle density, while a large maximum step size does not efficiently sample regions of high density.

5. DISCUSSION

Any Monte Carlo algorithm based on detailed balance is stochastically exact, i.e. it will, in the limit of an infinitely long run, produce convergence to the correct equilibrium averages. The problem is that runs are terminated after some finite number of steps, and this truncation leads to error, which is worse the slower the convergence rate of the algorithm [38]. This is why the efficiency of the algorithm is of real concern. As noted in the Introduction, in a previous application, on a dense, neat, Lennard-Jones liquid [37], a somewhat different version of DSMC resulted in slower convergence than MMC. Yet in the present application we find DSMC to be much faster than MMC. We explain this below.

There is an intrinsic inefficiency entailed in the use of a sampling cube whose size can vary. This comes from the need to reject all trial states from which one cannot, in one step, return to the original state, i.e. from the need to satisfy detailed balance by setting $a_{ij} = 0$ when $p_{ji}^* = 0$ (see equation 2 and the text after equation 5). In the present work the contribution to the rejection rate from this source was 0.204 (Table 2). For this reason, the convergence of our previous application of a variable sampling cube turned out to be relatively slow; any gain in speed from scaling the cube's size to the trial particle's potential energy was more than offset by this intrinsic loss. However, in the present application, where the density varies over 2 orders of magnitude, scaling the size of the cube according to the local density is so important a benefit, that it more than compensates for the above inefficiency.

Since the speed of DSMC in the present application stems from its ability to efficiently sample over a large density inhomogeneity, it is not difficult to think of other applications where DSMC would again be the algorithm of choice. For example, consider a Monte Carlo simulation on the liquid-vapour interface. Here again the physical system involves a large variation in density, this time through the interface. Clearly, this also should be an application where DSMC would be more effective than other Monte Carlo algorithms.

ACKNOWLEDGEMENTS

We are grateful to the Natural Sciences and Engineering Research Council of Canada for financial assistance, and the University of Guelph for its continuing support of the Special Computing Project and the Array Processor.

References

[1] M.T. Record, Jr., C.F. Anderson and T.M. Lohman, "Thermodynamic Analysis of ion effects on the binding and conformational equilibria of proteins and nuclei acids: the roles of ion association or release, screening and ion effects on water activity," *Q. Rev. Biophys.*, **11**, 103 (1978).

[2] M.T. Record, Jr., S.J. Mazur, P. Melançon, J.-H. Roe, S.L. Shaner and L. Unger, "Double Helical DNA: Conformations, Physical Properties, and Interactions with Ligands", *Ann. Rev. Biochem.*, **50**, 997 (1981).

[3] G.S. Manning, "The molecular theory of polyelectrolyte solutions with applications to the electrostatic properties of polynucleotides", *Q. Rev. Biophys.*, **11**, 179 (1978).
[4] F. Oosawa, *Polyelectrolytes*, Marcel Dekker, New York (1971).
[5] E. Sélégny, M. Mandel and U.P. Strauss, *Polyelectrolytes*, D. Reidel, Dordrecht (1974).
[6] S.A. Rice and M. Nagasawa, *Polyelectrolyte Solutions*, Academic Press, New York (1961).
[7] C.F. Anderson and M.T. Record, Jr., "The Thermodynamic Effects of Polyelectrolyte-Electrolyte Interactions", in *Structure and Dynamics: Nuclei Acids and Proteins*, E. Clementi and R.H. Sarma, eds., Academic Press, New York (1983).
[8] T.G. Wensel, C.F. Meares, V. Vlachy and J.B. Matthew, "Distribution of ions around DNA, probed by energy transfer", *Proc. Natl. Acad. Sci. U.S.A.*, **83**, 3267 (1986).
[9] C.T. Henningson, D. Karluk and P. Ander, "Comparison of Sodium Ion Interactions with Sodium Salts of (Carboxymethyl) cellulose and Vinylic Polyelectrolytes of varying charge density by Diffusion", *Macromolecules*, **20**, 1286 (1987).
[10] H.G. deJong, J. Lyklema and H.P. vanLeeuwen, "Conductometric analysis of the competition between monovalent and divalent counterions in their interaction with polyelectrolytes", *Biophysical Chemistry*, **27**, 173 (1987).
[11] A.R. Bizzari, C. Cametti and A. Di Basio, "Counterion Accumulation in Rod-like Polyelectrolyte Solutions with Added Salt and Manning's Condensation Theory", *Ber. Bunsenges. Phys. Chem.*, **92**, 17 (1988).
[12] G.S. Manning, "Limiting Laws and Counterion Condensation in Polyelectrolyte Solutions. I. Colligative Properties", *J. Chem. Phys.*, **51**, 924 (1969).
[13] G.S. Manning, "Counterion Binding in Polyelectrolyte Theory", *Acc. Chem. Res.*, **12**, 443 (1979).
[14] R.M. Fuoss, A. Katchalsky and S. Lifson, "The Potential of an infinite rod-like molecule and the distribution of the counter ions", *Proc. Natl. Acad. Sci. USA*, **37**, 579 (1951).
[15] M. Fixman, "The Poisson-Boltzmann equation and its application to polyelectrolytes", *J. Chem. Phys.*, **70**, 4995 (1979).
[16] C.W. Outhwaite, "A Modified Poisson-Boltzmann Equation for the Ionic Atmosphere around a Cylindrical Wall", *J. Chem. Soc., Faraday Trans. 2*, **82**, 789 (1986).
[17] A. Katchalsky, "Polyelectrolytes", *Pure and Appl. Chem.*, **26**, 327 (1971).
[18] A.D. MacGillivray, "Upper Bounds on Solutions of the Poisson-Boltzmann Equation near the limit of Infinite Dilution", *J. Chem. Phys.*, **56**, 80 (1972); "Analytic Description of the Condensation Phenomenon Near the Limit of Infinite Dilution Based on the Poisson-Boltzmann Equation", **56**, 83 (1972).
[19] R. Bacquet and P.J. Rossky", Ionic Atmosphere of Rod-like Polyelectrolytes. A Hypernetted Chain Study", *J. Chem. Phys.*, **88**, 2660 (1984).
[20] E. Gonzales-Tovar, M. Lozada-Cassou and D. Henderson, "Hypernetted chain approximation for the distribution of ions around a cylindrical electrode. II. Numerical solution for a model cylindrical polyelectrolyte", *J. Chem. Phys.*, **83**, 361 (1985).
[21] V. Vlachy and D.A. McQuarrie, "A Theory of cylindrical polyelectrolyte solutions", *J. Chem. Phys.*, **83**, 1927 (1985).
[22] W.G. McMillan and J.E. Mayer, "The statistical thermodynamics of multicomponent systems", *J. Chem. Phys.*, **13**, 276 (1945).
[23] H.L. Friedman and W.D.T. Dale, "Electrolyte Solutions at Equilibrium", in *Statistical Mechanics, Part A: Equilibrium Techniques*, B.J. Berne, ed., Plenum Press, New York, (1977).
[24] C.S. Murthy, R.J. Bacquet and P.J. Rossky, "Ionic Distributions near Polyelectrolytes. A Comparison of Theoretical Approaches", *J. Phys. Chem.*, **89**, 701 (1985).
[25] P. Mills, C.F. Anderson and M.T. Record, Jr., "Monte Carlo Studies of Counterion-DNA Interactions. Comparison of the Radial Distribution of Counterions with Predictions of Other Polyelectrolyte Theories", *J. Phys. Chem.*, **89**, 3984 (1985).
[26] V. Vlachy and A.D.J. Haymet, "A grand canonical Monte Carlo simulation study of polyelectrolyte solutions", *J. Chem. Phys.*, **84**, 5874 (1986).
[27] L.G. Nilsson, L. Nordenskiöld and Peter Stilbs, "Macroscopic Counterion Diffusion in Solutions of Cylindrical Polyelectrolytes. 2. Ion Correlation Effects", *J. Phys. Chem.*, **91**, 6210 (1987)
[28] D. Bratko and V. Vlachy, "Distribution of Counterions in the double layer around a cylindrical polyion", *Chem. Phys. Lett.*, **90**, 434 (1982).
[29] P.M. Mills, M.D. Paulsen, C.F. Anderson and M.T. Record, Jr., "Monte Carlo Simulations of Counterion Accumulation near Helical DNA", *Chem. Phys. Lett.*, **129**, 155 (1986).
[30] G.M. Torrie and J.P. Valleau, "Electrical double layers. I. Monte Carlo study of a uniformly charged surface," *J. Chem. Phys.*, **73**, 5807 (1980).
[31] N. Metropolis, A.W. Rosenbluth, M.N. Rosenbluth, A.H. Teller and E. Teller, "Equation of state

calculation by fast computing machines", *J. Chem. Phys.*, **21**, 1087 (1953).
[32] M. Rao, C. Pangali and B.J. Berne, "On the force bias Monte Carlo simulation of water: methodology, optimization and comparison with molecular dynamics", *Mol. Phys.*, **37**, 1773 (1979).
[33] C. Pangali, M. Rao and B.J. Berne, "On a novel Monte Carlo scheme for simulating water and aqueous solutions", *Chem. Phys. Lett.*, **55**, 413 (1978).
[34] P.J. Rossky, J.D. Doll and H.L. Friedman, "Brownian dynamics as smart Monte Carlo simulation", *J. Chem. Phys.*, **69**, 4628 (1978).
[35] S. Goldman, "A simple new way to help speed up Monte Carlo convergence rates: Energy-scaled displacement Monte Carlo", *J. Chem. Phys.*, **79**, 3938 (1983).
[36] S. Goldman, "Erratum to Ref. 35", *J. Chem. Phys.*, **84**, 1952 (1986).
[37] M. Mezei, K.A. Bencsath, S. Goldman and S. Singh, "The Detailed Balance Energy-scaled Displacement Monte Carlo Algorithm", *Molecular Simulation*, **1**, 87 (1987).
[38] J.P. Valleau and S.G. Whittington, "A Guide to Monte Carlo for Statistical Mechanics: 1. Highways", in *Statistical Mechanics, Part A: Equilibrium Techniques*, B.J. Berne, ed., Plenum Press, New York, (1979).